I&EC research
Industrial & Engineering Chemistry Research
pubs.acs.org/IECR
Article

A Hyphenated Approach Combining Pressure-Decay and *In Situ* FT-NIR Spectroscopy to Monitor Penetrant Sorption and Concurrent Swelling in Polymers

Valerio Loianno, Antonio Baldanza, Giuseppe Scherillo, Rezvan Jamaledin, Pellegrino Musto,* and Giuseppe Mensitieri

Cite This: *Ind. Eng. Chem. Res.* 2021, 60, 5494−5503

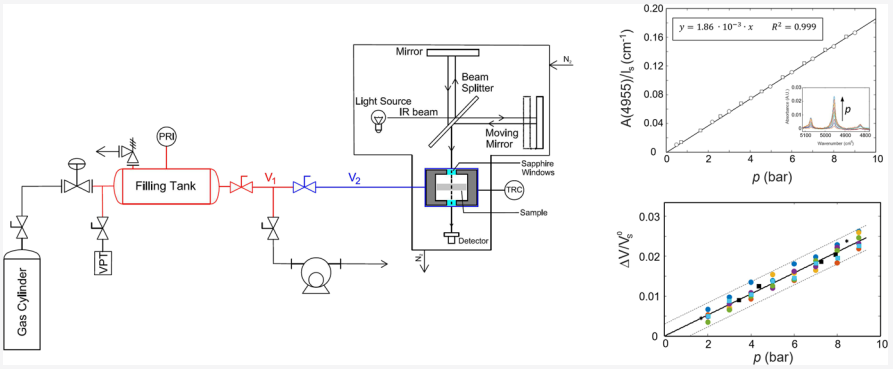

ABSTRACT: A new hyphenated technique based on simultaneous *in situ* FT-NIR spectroscopy and pressure-decay measurements has been implemented to study sorption of low-molecular-weight compounds in polymeric membranes and the induced swelling of the matrix. The FT-NIR measurements are performed in the transmission mode and, besides sorption equilibrium and kinetics, allow also the straightforward measurement of polymer swelling. The pressure decay method is used to provide quantitative information on the concentration of penetrant sorbed in the polymer. This measurement, once combined with the photometric data, allows an accurate estimation of the molar absorptivity of the analytical peaks as well. To validate the new experimental approach, sorption of CO_2 in polydimethylsiloxane at 35 °C and at pressures up to 9 bar has been investigated and the results are compared with available literature data.

1. INTRODUCTION

Nanofiltration, separation of gas mixtures in the oil & gas industry, and devolatization or addition of low-molecular-weight (M_W) compounds are just a few examples where polymeric materials are currently playing a significant role.[1,2] In particular, the interest for their use in the purification of chemical compounds stems from the global requirement of limiting both the production of greenhouse gases and the energy needed to perform the separation. For instance, in the US, it has been estimated that membrane-based separation processes would reduce by 90% the energy used as compared to thermal based unit operations (e.g., distillation) which amount approximately to 15.7 quad.[3] To successfully accomplish a separation, the polymeric material must be selected by taking into account the thermodynamic behavior of the polymer−penetrant mixture in the working conditions. Indeed, the solubility and the diffusivity of each species in the membrane strongly depend on the effects induced by the sorbed penetrant on the polymer, e.g., swelling, phase transitions, and physical and chemical degradation of the membrane.[4]

In this contribution, a new hyphenated approach, based on the combination of the pressure-decay technique and FT-NIR spectroscopy measurements in the transmission mode, has been implemented to achieve a thermodynamic characterization of the polymer−penetrant mixture. As a representative case, we have considered the sorption of carbon dioxide in polydimethylsiloxane (PDMS) at 35 °C and pressures up to 9 bar and the results have been compared with available literature data to validate the proposed approach.[5−7]

Received: January 19, 2021
Revised: March 25, 2021
Accepted: March 29, 2021
Published: April 8, 2021

https://doi.org/10.1021/acs.iecr.1c00264
Ind. Eng. Chem. Res. 2021, 60, 5494−5503

A barometric evaluation of sorption kinetics and equilibrium of gaseous CO_2 in PDMS as a function of pressure was done by pressure-decay measurements based on a molar balance. Concurrently, the polymer sample contained in the measuring cell was monitored by time-resolved FT-NIR while being exposed to the CO_2 admitted into the measuring cell. Subtraction spectroscopy methods were adopted to isolate the spectrum of sorbed carbon dioxide and to detect and quantify the dilation of the polymer matrix upon sorption. Comparison of the results of pressure-decay and vibrational spectroscopy measurements allowed the precise estimation of molar absorptivities of the probe molecule.

With reference to the dilation measurement, several approaches to measure polymer swelling have been proposed in the literature. Among them, Buckley et al.[8] implemented an optical method based on visible light, passing through a cell in which the specimen is in contact with the swelling solvent. Later, Wissinger and Paulaitis[9] used a cathetometer to measure the elongation of polymer specimens exposed to gaseous CO_2, with an estimated accuracy of ±0.03 mm. In the case of isotropic swelling, this measure allows an indirect estimate of the volume variation of the sample that resulted in an accuracy of 0.3% by volume.

Then, Fleming and Koros[10] proposed a new approach in which the sample is monitored with a CCD camera, evaluating the variation of each of the three specimen dimensions, thus allowing us to confirm the hypothesis of isotropic swelling for the PDMS−CO_2 system. Since then, this approach has become a standard.[11]

A further method consists in an ellipsometric measurement: Johnston et al.[12] pioneered this technique, which is, however, very accurate only for specimens whose thickness is lower than 2 μm. Another drawback is that the model for retrieving the film properties requires a large number of fitting parameters.[13]

Last, Kazarian and co-workers[14] were able to measure the polymer swelling via mid-FTIR spectroscopy in the ATR mode. They also used FT-NIR spectroscopy in the transmission mode to study the swelling of polymer samples contained in a CaF_2 cuvette.[15] However, this experimental approach is limited to liquid polymers and the sample is subjected to the physical constraints represented by the cuvette walls. The free-standing, unconstrained solid film used in the present experimental setup removes the above limitations. The hyphenated technique proposed in this contribution provides an alternative way for the measurement of polymer swelling at equilibrium based on the analysis of peaks associated with the polymer matrix. The quantitative evaluation of the absorbance variation allows an estimate of volume dilation, in the hypothesis of isotropic swelling. This approach overcomes several issues discussed above and offers additional advantages such as high sensitivity, flexibility, and the potential of measuring swelling concurrently with sorption kinetics and equilibrium.

2. THEORETICAL BACKGROUND

2.1. Sorption Kinetics of Low-Molecular-Weight Compounds in Rubbery Polymers. Usually, the evolution with time of the mass ($M(t)$) of a low M_W compound sorbed in a polymer film in contact with an external pure penetrant phase is described using the following simple empirical relationship at the initial stage:

$$M(t) = k \cdot t^n \tag{1}$$

where k and n are two fitting parameters. The behavior of the system is defined to be Fickian when n equals 0.5, case II for $n = 1$, and super case II for $n > 1$.[16]

In detail, Fick's law of diffusion successfully describes the kinetics of sorption of low M_W compounds in rubbery polymers, when the structural rearrangement of the macromolecules is faster than the mass transport itself. Conversely, anomalous or non-Fickian behavior is usually encountered in glassy polymers.[17] In the case of Fick's diffusive transport of a penetrant in a plane sheet of polymer, with constant thickness l_s^0 (that is, the sample thickness at the beginning of the sorption step), the instantaneous mass balance of the penetrant, subject to an abrupt concentration jump in the boundary conditions, admits the following analytical solution:[18]

$$\frac{M(t)}{M_\infty} = 1 - \sum_{n=0}^{\infty} \frac{8}{(2n+1)^2\pi^2} \exp\left[-\frac{D(2n+1)^2\pi^2 t}{(l_s^0)^2}\right] \tag{2}$$

It is noted that eq 2 refers to the case in which the penetrant concentration is so low that the mass-average velocity of the polymer−penetrant mixture can be considered negligibly small.[18] In eq 2, M_∞ is the mass of the penetrant within the polymer at equilibrium, and D is the penetrant−polymer mutual diffusivity, assumed to be independent of concentration (so called "ideal Fickian" behavior). In the case of a concentration-dependent diffusivity (so called "non-ideal Fickian" behavior), eq 2 can still provide a reasonable prediction of sorption kinetics by using, in place of D, an averaged diffusion coefficient, $\bar{D}$, defined as follows:

$$\bar{D} = \frac{1}{C_1 - C_2} \int_{C_1}^{C_2} D_{\text{eff}}(C)\mathrm{d}C \tag{3}$$

where C_1 and C_2 are the uniform concentrations of the penetrant inside the polymer slab at the beginning and the end of the experiment, respectively, and D_{eff} is the effective diffusion coefficient, which depends on the penetrant concentration. Moreover, it is worth noting that eq 2 is valid if the change of the thickness of the sample in the course of a sorption step is negligible as compared to the starting thickness of the sample.

In this work, both barometric measurements and *in situ* FT-NIR spectroscopy are used to study sorption kinetics. While in the pressure decay experiment, one obtains a direct estimate of $M(t)/M_\infty$, in the case of the spectroscopic measurement, based on the Lambert−Beer law and in the hypothesis of negligible volume dilation (≲3%), the sorption kinetics can be expressed in terms of absorbance as[19,20]

$$\frac{M(t)}{M_\infty} = \frac{A(t)}{A_\infty} \tag{4}$$

where $A(t)$ is the absorbance associated with the selected peak of carbon dioxide absorbed at time t within PDMS and A_∞ is the corresponding value at sorption equilibrium.

3. EXPERIMENTAL SECTION

3.1. Materials. Slabs of polydimethylsiloxane (PDMS) were prepared starting from Dow Corning Sylgard 184, a two-component silicone elastomer. The reactive mixture was degassed in a vacuum chamber for 30 min to remove air

https://doi.org/10.1021/acs.iecr.1c00264
Ind. Eng. Chem. Res. 2021, 60, 5494−5503

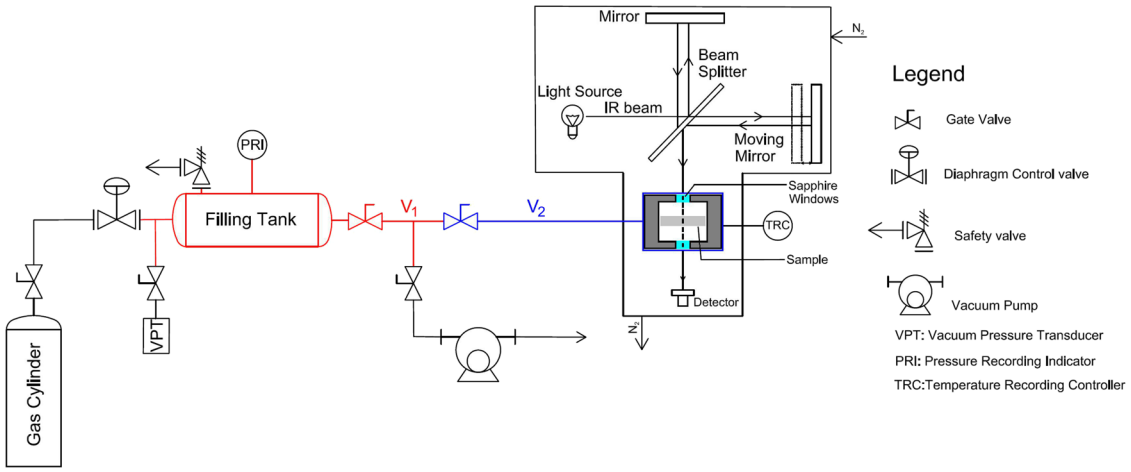

Figure 1. Schematic representation of the hyphenated apparatus.

bubbles generated by the mixing. Afterward, the mixture was poured on a Petri dish and cured overnight at 25 °C. Two slabs were tested, having correspondingly a thickness (l_s^0) of 1.50 ± 0.02 mm with a weight of 0.3000 g and 1.48 ± 0.02 mm with a weight of 2.000 g, as measured using a Mitutoyo IP65 digital micrometer with an accuracy ±0.002 mm. The density of the PDMS samples was measured by flotation in a mixture of water and $CaCl_2$ and is equal to 1.033 g/cm^3.

Carbon dioxide (purity of ≥99.995%) was purchased from Sol Group (Bologna, Italy). A pure water density standard (CAS number 7732-18-5) and anhydrous $CaCl_2$ (CAS number 10043-52-4) in the powder form with 99.99% purity were purchased from Sigma-Aldrich (Milan, Italy).

3.2. Pressure Decay Apparatus. The apparatus used to perform the hyphenated measurements is represented schematically in Figure 1. It consists of two chambers of known volume, i.e., a filling tank (the penetrant reservoir) and the measuring cell where the polymer sample is placed, separated by a shutoff valve. The valve is positioned at the top of the sample chamber in order to minimize the filling time during expansion. A pressure sensor, Baratron 121A from MKS instruments (Full Scale Pressure Range of 30 bar, accuracy of 0.5% of reading, resolution of 0.003 bar), is directly connected to the reservoir chamber (chamber 1 in Figure 1). The pressure of the apparatus when operating under vacuum (desorption steps) was measured using a Pirani vacuum gauge Adixen ATP 1004 (VPT in the figure) with an absolute pressure detection limit of 3 × 10^{-4} Torr. The whole system was tested to be leak-proof (connections are sealed using Swagelok VCR stainless steel gaskets), both under vacuum and at the highest investigated pressures.

The sample cell, made of 316 AISI stainless steel, is jacketed to allow thermal control by circulating thermostated water (resolution of temperature control of ± 0.01 °C using a HAAKE F6 bath). The cell is equipped with two coaxial windows made of sapphire (thickness of 2.25 mm) aligned with the IR beam. O-rings made of Viton guarantee that the windows are leak-tight. It has been verified, with *ad hoc* experiments, that the Viton O-rings do not interfere with pressure-decay measurement by possible sorption of a detectable amount of gas from the internal environment of the apparatus (see Figure S1, Supporting Information). The volumes of the different sections of the apparatus (see Figure 1 for volume labeling) have been measured using the Burnett method,[21] and the values are reported in Table 1. Volumes V_1 and V_2 have been evaluated by performing two expansions of gaseous carbon dioxide with and without a known volume of stainless steel spheres placed inside the filling tank. In Figure 1, volumes V_1 and V_2 are represented in red and in blue, respectively. Volume V_2 also includes the void volume of the shutoff valve that separates the sample chamber from the upstream volume V_1. The NIST database of thermophysical properties has been used to determine the compressibility factors for CO_2 at the chosen thermodynamic conditions.[22] The calibration measurements have been performed at 26.0 ± 0.1 °C. The Pirani vacuometer line is excluded from the volume calibration. The volume V_j of the jacketed section of the measuring cell has been estimated by measuring the volume of distilled water used to fill it. V_r is the difference between V_2 and V_j. The calculated volumes of the different sections of the apparatus are reported in Table 1.

Table 1. Measured Volumes of the Different Sections of the Experimental Apparatus

	V_1	V_2	V_j	V_r
volume (cm^3)	142.08 ± 0.03	63.94 ± 0.04	46.75 ± 0.06	17.19 ± 0.06

The accurate knowledge of these volumes is necessary to use the pressure-decay technique: indeed, sorption experiments were conducted at 35.0 ± 0.1 °C by controlling the temperature of the jacketed sample cell (V_j). The remaining parts of the apparatus were kept at 26.0 ± 0.1 °C. An *ad hoc* LabVIEW program was used to record the pressure and the temperature during time. The moles of carbon dioxide absorbed from the gas phase into the polymer have been calculated from the gas phase molar balance before expanding the gas in the sample chamber and after attaining sorption equilibrium. The NIST Thermophysical Properties Database has been accessed to evaluate the number of moles of carbon dioxide in the gas phase.[22]

The temperature non-uniformity has been taken into account to calculate the molar balance on the gas phase. A step discontinuity of the temperature value from 26 ± 0.1 to 35 ± 0.1 °C is assumed to be present at the junction between volume V_j and the remaining part of the apparatus (Figure 1). Consistently, the gas-phase molar balance is contributed by

https://doi.org/10.1021/acs.iecr.1c00264
Ind. Eng. Chem. Res. 2021, 60, 5494−5503

two terms, one related to the zone kept at 26 ± 0.1 °C and the other to the zone kept at 35 ± 0.1 °C.

3.3. FT-NIR Spectroscopy. To prevent atmospheric carbon dioxide from affecting the NIR measurements, N_2 was fluxed both in the FT-NIR instrument and along the path travelled by the IR beam outside the sample chamber. NIR measurements were performed in transmission mode with a Spectrum 100 spectrometer (Perkin Elmer, Norwalk, CT). The instrument is equipped with a germanium/KBr beam splitter and a wide band DTGS detector. To improve the time resolution in the sorption kinetic measurements, the following instrumental parameters were chosen: frequency resolution = 4 cm^{-1}; optical path difference velocity = 1 cm s^{-1}; spectral range = 8300−4000 cm^{-1}; one acquisition per spectrum. In these conditions, a single spectral collection took 0.9 s and was run in continuous. Conversely, when equilibrium was reached, the accuracy of the NIR spectrum was increased by fixing the parameters as follows: frequency resolution = 2 cm^{-1}; optical path difference velocity = 0.2 cm s^{-1}; spectral range = 8300−4000 cm^{-1}; number of co-added spectra = 16. The optical path length of the test chamber (L) was equal to 13.93 ± 0.01 mm. In the following, when the absorptivity will be retrieved from the peak height, the symbol ε (in cm^2/mol) will be used. Conversely, $\tilde{\varepsilon}$ will refer to the absorptivity related to the peak area (in km/mol). Sorption kinetics were collected by a dedicated software package for time-resolved measurements (*Timebase* from Perkin Elmer).

The absorbance spectrum of PDMS *in vacuo* was obtained using the empty cell as background, i.e.

$$A_p^0(\nu) = \frac{I_V(\nu)}{I_p^0(\nu)} \tag{5}$$

where $A_p^0(\nu)$ is the absorbance spectrum of the polymer matrix prior to the sorption test, I_p^0 and I_V are, respectively, the single-beam transmission spectra of the cell with and without the PDMS sample, both collected under a vacuum of 1.0 × 10^{-3} Torr. In an analogous fashion, the absorbance spectra of gaseous CO_2 at the investigated pressures were obtained with the same background $[I_V(\nu)]$, and with single beam spectra of the empty cell (i.e., without sample) at prescribed pressure values $[I^P_{CO_2}(\nu)]$. $A_p^0(\nu)$ and $A^0_{CO_2}(\nu)$ were used as reference spectra in difference spectroscopy to isolate the spectrum of carbon dioxide sorbed in the PDMS matrix (*vide infra*).

4. RESULTS AND DISCUSSION

4.1. Sorption Isotherm from Pressure Decay Measurements. Differential sorption measurements were performed at 35 °C by increasing stepwise the gas pressure in the test cell from 0 to 9 bar with a ΔP of around 1 bar. An integral sorption experiment (i.e., an experiment performed by stepping the CO_2 pressure directly from 0 to 6 bar) was also carried out. During the tests, the section of the apparatus occupying the volume $V_{tot} = V_1 + V_2 - V_j$ was kept at 26.0 ± 0.1 °C, while the jacketed cell (of volume V_j) was kept at 35 °C. A uniform pressure was established in the apparatus.

A typical pressure decay experiment was started by filling the volume V_1 (gas reservoir) with gas reaching a prescribed pressure. The remaining part of the apparatus, which includes the measuring cell, has a volume $V_2 - V_p$, where V_p is the volume of the polymer sample. At the start, this volume is either kept under vacuum, if one starts from a fully desorbed sample, or is at the final pressure of the previous sorption step. To start the test, the connecting valve was fully opened, allowing the expansion of the gas from a volume V_1 to a volume $V_1 + V_2 - V_p$. Pressure decay, due to sorption of CO_2 within the polymer, was monitored as a function of time, until a constant equilibrium value was attained (see Figure S1, Supporting Information). Knowing the values of the initial pressure in volume V_1 and in volume $V_2 - V_p$ and of the final pressure in the total volume of the apparatus, $V_1 + V_2 - V_p$, one can perform a molar balance. By comparing the number of moles of gas initially present with the corresponding final value, one can determine the amount of gas sorbed in the polymer at equilibrium. The carbon dioxide isotherm in PDMS determined using this procedure is presented in Figure 2 along

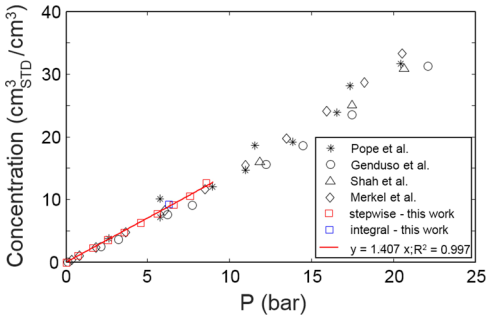

Figure 2. Sorption isotherm of CO_2 in PDMS at 35 °C. Data from the literature were measured by barometric techniques.

with data available in the literature. The measurement error has been estimated by taking into account the error inherent in the volume calculation during calibration, and in the temperature, pressure, and specimen density measurements. The propagation of these errors on the concentration was estimated to be equal to about 5% of each concentration value.

As expected, the trend is linear in the pressure range investigated and the concentration values are in excellent agreement with the literature data.

In designing their dual volume−variable pressure system, Koros and Paul pointed out that, to guarantee the maximum accuracy, the volumes of the two sections of the apparatus should be approximately equal.[23] Indeed, the present apparatus can be easily arranged to fulfill this requirement, thus allowing reliable measurements also with polymeric materials with a lower gas solubility. For instance, using a PDMS specimen of 2.0034 g, the volume ratio $\frac{V_1}{V_2 - V_p}$ is ≅ 2.29. This value is low enough to prevent scattering, and it can be further reduced down to approximately 1.63, lowering the V_1 value by filling the upstream chamber with stainless steel spheres.

The determination of the sorption isotherm can be also performed by using infrared spectroscopy, once the value of the molar absorptivity associated with the selected analytical peaks is available, as is described in detail in the following. The proposed hyphenated technique allows the straightforward estimation of this quantity by comparing peak absorbance at equilibrium with equilibrium gas concentration within the polymer measured by the pressure decay technique, in the same conditions.

4.2. FT-NIR. In the present application, the photometric monitoring of sorption equilibrium and kinetics requires a technique capable of providing quantitative information on specimens having thicknesses above the millimeter. FT-NIR is well suited for the purpose since the non-fundamental modes

https://doi.org/10.1021/acs.iecr.1c00264
Ind. Eng. Chem. Res. 2021, 60, 5494−5503

(overtones and combinations) that are observed in the 10,000−4000 cm^{-1} range exhibit low cross-sectional values (i.e., small molar absorptivity) compared to the fundamental vibrations in the mid-IR (4000−400 cm^{-1}). In fact, all bands in the NIR spectrum of the PDMS sample, except the strongest at 4359 cm^{-1}, lie within 1.5 absorbance units (*cf* Table 2). In this absorbance interval, the Beer−Lambert relationship is generally fulfilled,[24] allowing accurate and reproducible quantitation.

Table 2. Observed Frequencies, Intensities, and Assignments for the NIR Spectrum of PDMS

peak frequency (cm^{-1})	absorbance at 1.50 mm (A.U.)	mode
7305	0.05	$2\nu_{as}(CH_3) + \delta_{as}(CH_3)$
7127	0.08	$\nu_s(CH_3) + 3\delta_{as}(CH_3)$
5916	0.44	$2\nu_{as}(CH_3)$
5873	0.47	$2\nu_s(CH_3)$
5724	0.44	$2\nu_s(CH_3) + \nu_s(CH_3) + 2\delta_{as}(CH_3)$
5605	0.14	$\nu_{as}(CH_3) + \delta_s(CH_3) + \delta_{as}(CH_3)$
5447	0.09	$\nu_{as}(CH_3) + 2\delta_s(CH_3)$
5402	0.10	$\nu_s(CH_3) + 2\delta_s(CH_3)$
4359	2.19	$\nu_{as}(CH_3) + \delta_{as}(CH_3)$
4216	1.28	$\nu_{as}(CH_3) + \delta_s(CH_3)$
4163	0.50	$\nu_s(CH_3) + \delta_s(CH_3)$
4050	0.51	$2\delta_a(CH_3) + \delta_s(CH_3)$

The blue trace in Figure 3A represents the PDMS spectrum *in vacuo*, that is, the spectrum obtained using the background

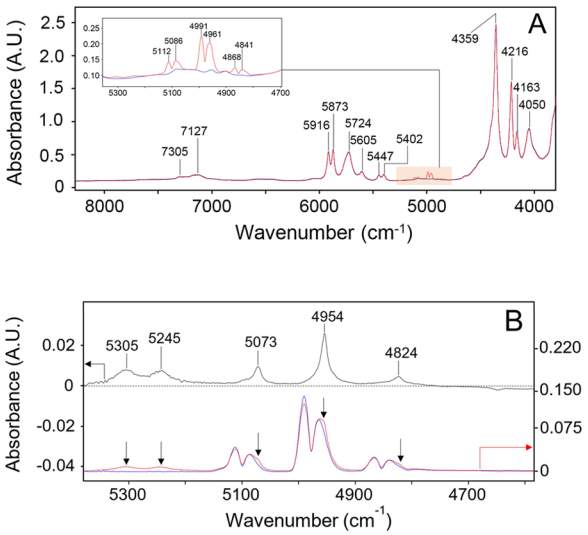

Figure 3. (A) Blue trace: FT-NIR spectrum of PDMS under vacuum; red trace: FT-NIR spectrum of PDMS equilibrated at a CO_2 pressure of 9 bar. The inset highlights the analytical range (5320−4700 cm^{-1}). (B) Red trace: difference between the spectrum at CO_2 pressure = 9 bar and the spectrum under vacuum (k = 1); blue trace: gas-phase spectrum of CO_2 at 9 bar; black trace: difference spectrum (red trace − k blue trace).

collected on the empty cell under vacuum. It is dominated by the vibrations involving the hydrogen atom due to their pronounced anharmonicity. In fact, all bands, except those at 5916, 5873, and 4050 cm^{-1}, are combinations of CH_3 stretching and CH_3 bending modes. The doublet at 5916−5873 cm^{-1} is due to the first overtone of the two CH_3 stretches. The 4050 cm^{-1} band originates from a combination of the symmetric and antisymmetric bending of the same unit. A detailed assignment of the observed bands to the associated vibrational transitions[25] is reported in Table 2.

Since the NIR bands originate solely from the methyl group, it can be supposed that the PDMS spectrum will not be perturbed by any interaction of the polymer matrix with the probe molecule, which may eventually involve the oxygen atom of the siloxane group. The NIR spectrum is therefore expected to remain inert upon CO_2 sorption. Actually, in the forthcoming paragraph, we will see this anticipation to be incorrect; the interpretation of the observed effects will provide further information.

The red trace in Figure 3A corresponds to the NIR spectrum of PDMS after injection of 9 bar of CO_2 and successive equilibration. It contains, therefore, the signals of gaseous CO_2 and those of carbon dioxide dissolved in the polymer matrix, which is in a condensed state. The two sets of signals are expected to be clearly discernible, due to the removal of the rotovibrational fine structure in the condensed phase. The only signals attributable to CO_2 occur in the 4800−5400 cm^{-1} interval (*cf* the inset of Figure 3A). In this range is observed the CO_2 Fermi triad, consisting of three R−P profiles due, correspondingly, to the $(4\nu_2 + \nu_3)$ transition at 4853 cm^{-1}, the $(\nu_1 + 2\nu_2 + \nu_3)$ transition at 4978 cm^{-1}, and the $(2\nu_1 + \nu_3)$ transition at 5100 cm^{-1}.[26,27] At 9 bar, the maximum intensity lies below 0.15 A.U.; this value—well within the sensitivity range of the technique—indicates that the available pressure interval can be extended at least to 30 bar. The spectrum of PDMS in the analytical range is featureless, showing only a non-specific background absorption. By removing the polymer contribution, a consistent zero baseline is obtained, which improves the quantitative analysis (*cf* Figure 3B, red trace). The polymer component of the NIR spectrum can be suppressed in two ways: (i) by using the single-beam spectrum of the polymer under vacuum as the background and (ii) by subtracting the absorbance spectrum of the polymer under vacuum from the absorbance spectrum of the polymer in contact with CO_2 (see Experimental Section). If the subtraction factor k is taken equal to unity, the two approaches are equivalent. In fact, they differ for the consideration of potential volumetric effects. The first (ratio method[28,29]) ignores these effects; the second (difference spectroscopy)[24,28,30] may or may not take into account the changes occurring in the sample dimensions. In any case, these changes are quantitatively reflected in the photometric observables, as will be discussed in detail in the forthcoming paragraph.

Figure 3B compares the CO_2 spectrum at a pressure of 9 bar, with and without the PDMS sample in the test chamber (red and blue traces, respectively). The contribution of the carbon dioxide dissolved in the polymer matrix reveals itself in the form of well-defined shoulders in the right side of the P-branches of the three transitions (highlighted by vertical arrows in Figure 3B). The CO_2 spectrum in the condensed phase can be isolated by subtracting out the blue from the red trace and adjusting the k factor so as to reduce the Fermi triad to the zero baseline. The result of this analysis is represented in Figure 3B, black trace.

Formally

https://doi.org/10.1021/acs.iecr.1c00264
Ind. Eng. Chem. Res. 2021, 60, 5494−5503

$$A_d(\nu) = A_s(\nu) - k\cdot A_r(\nu) = [A_{gas}(\nu) + A_{cd}(\nu)] - k\cdot A'_{gas}(\nu) = l\cdot\left[\frac{p}{ZRT}\cdot\varepsilon_{gas}(\nu) + C_{cd}\cdot\varepsilon_{cd}(\nu)\right] - k\cdot L\cdot\frac{p}{ZRT}\cdot\varepsilon_{gas}(\nu) \quad (6)$$

In eq 6, A_d, A_s, and A_r are, respectively, the difference, the sample, and the reference spectra expressed in absorbance units; k is the subtraction factor; A_{gas} and A_{cd} are the gas-phase and the condensed-phase spectra of carbon dioxide for the test performed at a CO_2 pressure of p bar; A'_{gas} is the spectrum of CO_2 in the gas phase collected at p bar in the empty cell (i.e., without the sample); $Z(p,T)$ is the compressibility factor; C_{cd} is the concentration of CO_2 in the polymer matrix (mol/cm^3); ε_{gas} and ε_{cd} are the molar absorptivities of the gas and the condensed phase, respectively; l and L are the optical path lengths of the test chamber with and without the sample, with $l = L - l_0 \cong L - l_s^0$, l_s^0 being the initial sample thickness. Adjusting k to null the gas phase spectrum gives $k = (L - l_s^0)/L$. Due to the reduction of the optical path length, the gas phase spectrum is more intense in the absence than in the presence of the PDMS sample in the test chamber, as shown in Figure 3A (*cf* the R branch at 4991 cm^{-1} in the blue and red traces).

The k value to produce the difference spectrum of Figure 3B (black trace) amounts to 0.890, which, associated with the path length of the test chamber (13.93 mm), provides an estimated sample thickness of 1.50 ± 0.04 mm, in good agreement with the measured value of 1.48 mm. This result is a useful cross-check for the proposed multistep processing of the spectral data and confirms the soundness of the analytical approach. Equation 6 predicts k to be independent from CO_2 pressure; in fact, in the whole p range, very consistent k values were obtained, averaging to 0.900 with a standard deviation of 0.008.

The NIR spectrum of condensed CO_2, isolated by difference spectroscopy, displays three sharp peaks at 5073, 4954, and 4824 cm^{-1}, corresponding to the Fermi triad with frustrated rotovibrational transitions. The three lineshapes are coincident and, according to the general theory of vibrational line profiles,[31,32] can be described by the sum of a Gaussian and a Lorentzian component both centered at the peak maximum. The appropriateness of the theoretical model to simulate the 4954 cm^{-1} band shape is demonstrated in Figure 4, which also confirms that the proposed data analysis isolates correctly the signal of interest. The two-component structure is interpreted assuming the Gaussian part as being remnant of the gas-phase spectrum, while the sharp, Lorentz-like component is the purely vibrational transition active in the condensed phase (but not in the gas phase).[33,34] More specifically, the composite band shape is the consequence of the probe dynamics within the molecular environment, i.e., free rotation in the early stages of the relaxation process (0.2−1.0 ps), which produces the Gaussian component, and random rotational diffusion at later stages (the so-called Debye regime), giving rise to the Lorentz component. The well-developed Gaussian component is indicative of a sizeable free-rotation regime, which, in turn, suggests that the probe senses a poorly interactive or non-interactive environment. A more quantitative analysis of the band shape is beyond the scope of the present study and will be discussed in a forthcoming contribution.

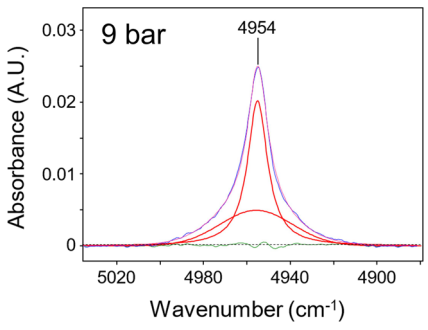

Figure 4. Curve fitting analysis of the CO_2 band at 4954 cm^{-1}. Blue trace: experimental spectrum; purple trace: best-fitting result; red traces: resolved components; green trace residual (experimental − best-fit).

A further intriguing observation is the appearance of a weak doublet at 5303−5245 cm^{-1} (*cf* Figure 3B, black trace and Figure 8A, top panel); the intensity of this profile increases linearly with the amount of sorbed CO_2 (see Figure S2A,B, Supporting Information), suggesting that the couple of signals is produced by the probe. On the other hand, there are no corresponding transitions in the gas-phase spectrum of CO_2 and the band shapes are considerably different from those of the Fermi triad in the condensed phase. One possible interpretation is that the doublet originates from a small fraction of CO_2 molecules interacting with specific sites on the polymer backbone (possibly, the oxygen atoms of the siloxane unit), but presently, this hypothesis is to be considered speculative. Work is in progress to elucidate this relevant aspect.

Figure 5 shows the sorption isotherm evaluated photometrically from the height of the peak at 4955 cm^{-1}. The linearity exceeds 0.999; the measurement is accurate and reproducible, as demonstrated by the consistency of two data sets collected on samples with different thicknesses.

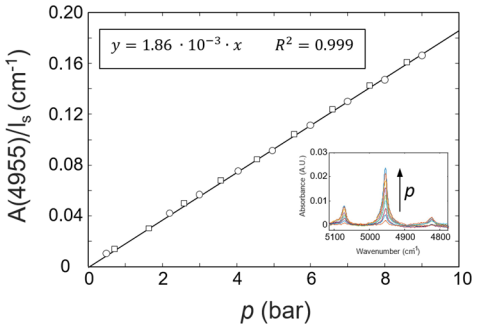

Figure 5. Sorption isotherm as measured by FT-NIR spectroscopy from the absorbance of the CO_2 band at 4955 cm^{-1}. circle, open: sample thickness = 1.50 mm; square, open: sample thickness = 1.48 mm.

The correlation between photometric and pressure decay data is reported in Figure 6. The diagram confirms the validity of the Beer−Lambert law (R^2 = 0.997) and illustrates the potential of the proposed hyphenated approach for measuring accurate values of molar absorptivity. The knowledge of this physical constant not only enables one to perform precise quantitative analysis but also provides relevant information on the molecular environment interrogated by the probe. In fact,

https://doi.org/10.1021/acs.iecr.1c00264
Ind. Eng. Chem. Res. 2021, 60, 5494−5503

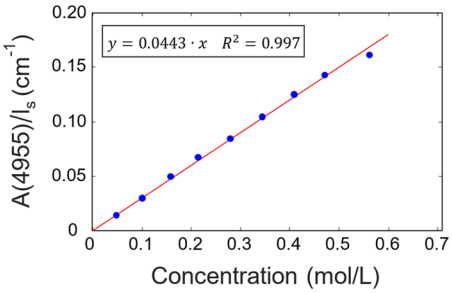

Figure 6. Correlation between the concentration of sorbed CO_2 measured by pressure decay and the absorbance of the CO_2 band at 4955 cm^{-1}.

the absorptivity is related to the polarity of the vibrating unit according to[35]

$$\tilde{\varepsilon}(\nu) = \int_{\nu_1}^{\nu_2} \varepsilon(\nu)\mathrm{d}\nu = \frac{1}{2.3}\cdot\frac{\pi N_A}{3c^2\mu_{red}}\cdot\left(\frac{\partial\vec{\mu}}{\partial Q_i}\right)^2_{Q_i=0} \quad (7)$$

where N_A is the Avogadro number, μ_{red} is the reduced mass of the oscillator, c is the speed of light and $(\partial\vec{\mu}/\partial Q_i)$, the derivative of the dipole moment with respect to the ith normal coordinate, is the transition moment . The quadratic dependence of $\tilde{\varepsilon}$ on the transition moment makes this quantity very sensitive to any perturbation of the electron density distribution within the molecular structure. Thus, $\tilde{\varepsilon}$ shows to be highly responsive to the formation of molecular interactions between the probe and the polymer matrix, much more than peak shifts, that are the parameters customarily employed to detect and investigate these effects. In Table 3 are reported the

Table 3. Molar Absorptivities of the Investigated CO_2 Peaks

peak at 5073 cm^{-1}		peak at 4954 cm^{-1}		peak at 4824 cm^{-1}	
ε(cm^2/mol)	$\tilde{\varepsilon}$ (km/mol)	ε (cm^2/mol)	$\tilde{\varepsilon}$ (km/mol)	ε (cm^2/mol)	$\tilde{\varepsilon}$ (km/mol)
99.65	0.02201	299	0.06628	37.22	0.007452

molar absorptivity values of the components of the Fermi triad in the PDMS medium. The absorbance vs concentration curves for the Fermi triad are compared in the Supporting Information (see Figure S3).

The experimental approach proposed in the present study is equally suited for measuring sorption kinetics. This is demonstrated in Figure 7A, which shows the spectroscopic monitoring of the integral sorption step 0−5.976 bar on the specimen 1.50 mm thick. Pressure lowering due to sorption during the experiment determines a change of boundary conditions to which the sample is exposed. However, because of the low mass of the specimen, this change is negligible for the purposes of the kinetics analysis that has been performed assuming time-invariant boundary conditions. The behavior is Fickian, and the kinetics is well described by the classical diffusion process in a slab of thickness l_s. The diffusivity of CO_2 in PDMS at 35 °C and at an average concentration of 0.171 mol L^{-1} is 1.9 × 10^{-5} cm^2 s^{-1}. The desorption process is also Fickian (see Figure S4, Supporting Information) and the diffusivity evaluated therefrom is close to the value from the sorption experiment, thus indicating that, as expected, this parameter is rather independent on CO_2 concentration.[18] The diffusivity value determined in the present study is consistent with that reported by Merkel et al.,[6] obtained from independent permeability and solubility measurements (i.e., 1.8 × 10^{-5} cm^2 s^{-1}).

In Figure 7B are compared the results obtained with the two techniques for the differential sorption test from 4.555 to 5.569 bar. The matching of the two data sets is satisfactory, albeit the pressure-decay measurement approaches its limiting sensitivity. The signal to noise ratio for the latter technique can be, however, improved using a higher amount of PDMS and/or by reducing the gas phase volume.

4.3. Spectroscopic Monitoring of the Sorption Induced Swelling. Since the signal intensity in NIR spectroscopy is linearly related to the sample thickness and the volumetric concentration of the oscillator, it could be possible, in principle, to quantitatively evaluate the geometrical parameters of a polymer sample during penetrant sorption by spectroscopic means. Peaks used for this purpose must fulfill several requirements: ideally, they are well-resolved, display a simple, symmetrical band shape, and are not perturbed by molecular interactions with the probe. The latter is a necessary condition, since only in this case the observed perturbation of the peak intensity can be entirely ascribed to a volumetric effect. The first two requirements are less stringent: non-ideal cases can be handled by use of data analysis tools like difference spectroscopy and/or least-squares curve fitting (*vide infra*).

Absorbance is related to volume dilation according to

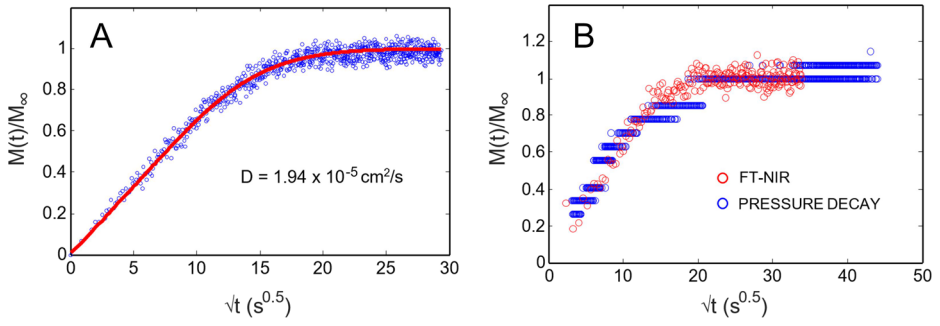

Figure 7. (A) Sorption kinetics evaluated spectroscopically from the peak absorbance at 4955 cm^{-1}. Integral sorption test at $p(CO_2)$ = 0−5.976. The blue symbols are the FT-NIR data; the continuous line represents the best fitting provided by the second Fick law (eq 2). (B) Comparison between sorption kinetics evaluated spectroscopically (red dots) and by pressure decay (blue dots). Differential sorption test at $p(CO_2)$ = 4.555−5.569 bar.

https://doi.org/10.1021/acs.iecr.1c00264
Ind. Eng. Chem. Res. 2021, 60, 5494−5503

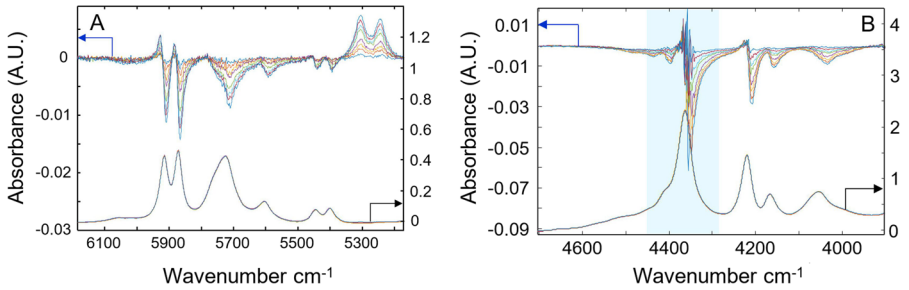

Figure 8. (A) Absorbance spectra (bottom panels) and difference spectra (top panels) in two frequency ranges for the PDMS sample equilibrated at different CO_2 pressures. Blue trace: p = 2 bar; red: p = 3 bar; orange: p = 4 bar; purple: p = 5 bar; green: p = 6 bar; light blue: p = 7 bar; brown: p = 8 bar; dark blue: p = 9 bar. The absorbance panels also contain the spectrum collected under vacuum for reference (black trace). (B) Shaded area highlighting the case of a band whose intensity goes beyond the linearity range (2.4. absorbance units). Exceeding the intensity threshold reflects clearly in the difference spectra.

$$A_p^0 = \varepsilon_p l_s^0 C_p^0 = \varepsilon_p l_s^0 \frac{n_p}{V_s^0} = \varepsilon_p \frac{n_p}{h_s^0 \cdot w_s^0} \tag{8}$$

$$A_p^{eq} = \varepsilon_p (l_s^0 + \Delta l_s) C_p^{eq} = \varepsilon_p (l_s^0 + \Delta l_s) \frac{n_p}{V_s^{eq}} = \varepsilon_p \frac{n_p}{(h_s^0 + \Delta h)(w_s^0 + \Delta w)} \tag{9}$$

where A_p^0 and V_s^0 are, respectively, the absorbance of the selected polymer peak and the volume of the sample at the beginning of the sorption experiment, A_p^{eq} and V_s^{eq} refer to the same quantities at sorption equilibrium, ε_p is the molar absorptivity of the analytical peak, C_p^0 and C_p^{eq} are the initial and the equilibrium polymer densities expressed in terms of molar concentration of repeating units, n_p is the number of moles of repeating units in the sample volume, and h_s^0 and w_s^0 are the height and width of the sample at the beginning of the sorption experiment.

For the invariance of the polymer mass in the sorption experiment and assuming small displacements with respect to the initial dimensions, eqs 8 and 9 can be rewritten as

$$\frac{A_p^0}{A_p^{eq}} = \frac{(h_s^0 + \Delta h)(w_s^0 + \Delta w)}{h_s^0 w_s^0} \cong 1 + 2\frac{\Delta h}{h_s^0} \tag{10}$$

Finally, for systems behaving isotropically (i.e., when $\Delta l_s/l_s^0 = \Delta h/h_s^0 = \Delta w/w_s^0$), which is the case of PDMS, as confirmed by several studies,[10,36] the relationship between absorbance and volume dilation becomes

$$\frac{\Delta V}{V_s^0} \cong 3\frac{\Delta h}{h_s^0} \cong \frac{3}{2}\left(\frac{A_p^0}{A_p^{eq}} - 1\right) \tag{11}$$

Equation 11 predicts that volume dilation produces a decrease of peak intensities. The whole NIR spectrum is suitable for swelling analysis for it originates from methyl group vibrations (see Table 2) and is therefore inert toward any molecular interaction. Thus, we have considered all the features in the 6200−5200 and the 4800−3900 cm^{-1} ranges, except the band at 4359 cm^{-1}, which lies above the linearity range. The doublet at 7305−7127 cm^{-1} is too weak to provide reliable results. The effect induced by swelling on the absorbance spectrum of PDMS is barely detectable, as can be seen in Figure 8A,B, bottom panels, which display the traces collected on the sample equilibrated at different pressures in the two analytical ranges. An effective method for highlighting subtle effects is difference spectroscopy: in the present application, the spectrum of the PDMS sample collected under vacuum is used as reference and directly subtracted (i.e., using k = 1) from the spectra of the sample equilibrated at increasing p values. Swelling reveals itself in the form of negative peaks with respect to the zero baseline, occurring at positions corresponding to the original absorbance features. The intensity of the peaks in the difference spectrum ($\Delta A_p = A_p^{eq} - A_p^0$) can be plugged into eq 11 after slight rearrangement:

$$\frac{\Delta V}{V_s^0} \cong \frac{3}{2}\left(\frac{A_p^0}{\Delta A_p + A_p^0} - 1\right) \tag{12}$$

which requires the A_p^0 value to provide the desired dimensional information. Equation 12 is useful whenever the analytical peak(s) is not fully resolved, as in the present case. In fact, difference spectroscopy significantly improves the resolution (see Figure 8A,B, top panels) while the A_p^0 value, to be obtained by LSCF analysis, is only required for the reference spectrum (*cf* Figure S5, Supporting Information).

The swelling results, evaluated by considering the peaks of the difference spectra located at 5867, 5650, 5595, 4155, and 4035 cm^{-1}, are presented in Figure 9. Whenever possible, i.e., when the peak is fully resolved and has a sharp lineshape indicative of a single-component structure (i.e., at 5867, 5595, and 4157 cm^{-1}), the peak height was used for intensity evaluation. Otherwise, the analysis was performed by use of the peak area (i.e., at 5650 and 4035 cm^{-1}). The $\Delta V/V_s^0$ vs p diagram, represented in Figure 9, is highly linear (y = 0.002634

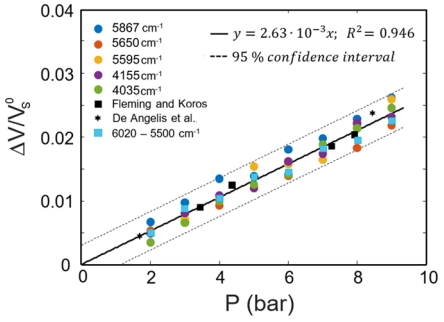

Figure 9. Swelling of PDMS upon CO_2 sorption measured spectroscopically as a function of CO_2 pressure. Data evaluated from different spectral features, as indicated. Literature data from refs 10 (square, closed) and 37 (star, closed) are also reported for comparison.

https://doi.org/10.1021/acs.iecr.1c00264
Ind. Eng. Chem. Res. 2021, 60, 5494−5503

· x; R^2 = 0.946), with all points tightly and randomly distributed around the straight line regressed from the whole data set. In particular, every data point falls within the 95% confidence interval calculated for the best-fitting line. The agreement with literature results is also excellent;[10,37] as shown in Figure 9, literature data line up exactly on our regression result. The noise observed in the difference spectra (Figure 8) does not affect significantly the swelling data; it has been estimated, by an *ad hoc* Monte Carlo simulation, to be lower than 1%. The larger scattering observed for some signals is to be attributed to baseline fluctuations in the analytical interval.

The results reported in Figure 9 validate on quantitative grounds the hypothesis that the observed decrease of absorbance is to be entirely ascribed to volumetric effects and, as such, is independent of peak frequency. This allows us to simplify the swelling analysis by considering a whole set of peaks in a specific frequency range, thus avoiding difference spectroscopy and curve fitting analysis. As an example, in Figure 9, the cyan square symbols refer to data evaluated by considering the integral over the 6020−5500 cm^{-1} interval. The results are accurate and display minimum scattering, on account of a reliable baseline and a substantial intensity. It is noted, however, that the possibility of employing an extended frequency range with a multiplicity of spectral features is rather an exception than a common occurrence. In the case of PDMS, this possibility stems from the vibrational character of the NIR spectrum, solely generated by the inert methyl groups. In general, especially when working in the mid-IR, this situation is rarer. In any case, the absence of spurious (i.e., interactional and/or conformational) effects is to be carefully verified prior to attempting the integral approach.

5. CONCLUSIONS

A novel hyphenated technique based on pressure-decay and FT-NIR spectroscopy measurements is presented, which allows the concurrent monitoring of sorption kinetics and equilibria and sorption-induced swelling. The proposed experimental approach provides accurate and reproducible data that are successfully compared with literature results. In particular, the photometric swelling measurements show a remarkable sensitivity of 0.5% by volume. The possibility of recording simultaneously absolute concentration values and photometric data allows the accurate determination of molar absorptivities, which are essential reference values for the numerous industrial applications of NIR univariate analysis (materials characterization, on-line process control, and more). In a more fundamental perspective, molar absorptivities bring about relevant information on the molecular environment surrounding the probe and on its interactive character.

■ ASSOCIATED CONTENT

Supporting Information

The Supporting Information is available free of charge at https://pubs.acs.org/doi/10.1021/acs.iecr.1c00264.

Pressure-decay measurement, FT-NIR spectra of PDMS, FT-NIR calibrations, desorption kinetics, curve fitting analysis, details on the experimental protocol (PDF)

■ AUTHOR INFORMATION

Corresponding Author

Pellegrino Musto − *Institute for Polymers, Composites and Biomaterials, National Research Council of Italy, Pozzuoli 80078, Italy;* orcid.org/0000-0001-6307-1410; Email: pellegrino.musto@cnr.it

Authors

Valerio Loianno − *Dept. of Chemical, Materials and Production Engineering, University of Naples Federico II, Naples 80125, Italy*

Antonio Baldanza − *Dept. of Chemical, Materials and Production Engineering, University of Naples Federico II, Naples 80125, Italy*

Giuseppe Scherillo − *Dept. of Chemical, Materials and Production Engineering, University of Naples Federico II, Naples 80125, Italy*

Rezvan Jamaledin − *CABHC@CRIB, Istituto Italiano di Tecnologia, Naples 80125, Italy;* orcid.org/0000-0003-2389-3393

Giuseppe Mensitieri − *Dept. of Chemical, Materials and Production Engineering, University of Naples Federico II, Naples 80125, Italy; Institute for Polymers, Composites and Biomaterials, National Research Council of Italy, Pozzuoli 80078, Italy;* orcid.org/0000-0001-9333-0292

Complete contact information is available at: https://pubs.acs.org/10.1021/acs.iecr.1c00264

Author Contributions

V.L.: sample characterization, conceptualization, and experiments execution; G.S. and A.B.: data processing and numerical calculations; R.A.: sample preparation and characterization; P.M.: spectroscopic analysis, supervision, and writing; G. M.: supervision and writing. All authors have given approval to the final version of the manuscript.

Notes

The authors declare no competing financial interest.

■ ACKNOWLEDGMENTS

Thanks are due to Mr. G. Orefice for assistance in performing the FT-NIR measurements.

■ REFERENCES

(1) Galizia, M.; Bye, K. P. Advances in organic solvent nanofiltration rely on physical chemistry and polymer chemistry. *Front. Chem.* **2018**, *6*, 511.

(2) Galizia, M.; Chi, W. S.; Smith, Z. P.; Merkel, T. C.; Baker, R. W.; Freeman, B. D. *50th Anniversary Perspective*: Polymers and Mixed Matrix Membranes for Gas and Vapor Separation: A Review and Prospective Opportunities. *Macromolecules* **2017**, *50*, 7809−7843.

(3) Sholl, D. S.; Lively, R. P. Seven chemical separations to change the world. *Nature* **2016**, *532*, 435−437.

(4) Pierleoni, D.; Minelli, M.; Scherillo, G.; Mensitieri, G.; Loianno, V.; Bonavolontà, F.; Doghieri, F. Analysis of a Polystyrene−Toluene System through "Dynamic" Sorption Tests: Glass Transitions and Retrograde Vitrification. *J. Phys. Chem. B* **2017**, *121*, 9969−9981.

(5) Shah, V. M.; Hardy, B. J.; Stern, S. A. Solubility of carbon dioxide, methane, and propane in silicone polymers: effect of polymer side chains. *J. Polym. Sci., Part B: Polym. Phys.* **1986**, *24*, 2033−2047.

(6) Merkel, T. C.; Bondar, V. I.; Nagai, K.; Freeman, B. D.; Pinnau, I. Gas sorption, diffusion, and permeation in poly(dimethylsiloxane). *J. Polym. Sci., Part B: Polym. Phys.* **2000**, *38*, 415−434.

(7) Genduso, G.; Litwiller, E.; Ma, X.; Zampini, S.; Pinnau, I. Mixed-gas sorption in polymers *via* a new barometric test system: Sorption and diffusion of CO_2-CH_4 mixtures in polydimethylsiloxane (PDMS). *J. Membr. Sci.* **2019**, *577*, 195−204.

(8) Buckley, D. J.; Berger, M.; Poller, D. The swelling of polymer systems in solvents. I. Method for obtaining complete swelling−time curves. *J. Polym. Sci.* **1962**, *56*, 163−174.

(9) Wissinger, R. G.; Paulaitis, M. E. Swelling and sorption in polymer−CO_2 mixtures at elevated pressures. *J. Polym. Sci., Part B: Polym. Phys.* **1987**, *25*, 2497−2510.
(10) Fleming, G. K.; Koros, W. J. Dilation of polymers by sorption of carbon dioxide at elevated pressures. 1. Silicone rubber and unconditioned polycarbonate. *Macromolecules* **1986**, *19*, 2285−2291.
(11) Moon, J. D.; Galizia, M.; Borjigin, H.; Liu, R.; Riffle, J. S.; Freeman, B. D.; Paul, D. R. Water vapor sorption, diffusion, and dilation in polybenzimidazoles. *Macromolecules* **2018**, *51*, 7197−7208.
(12) Sirard, S. M.; Ziegler, K. J.; Sanchez, I. C.; Green, P. F.; Johnston, K. P. Anomalous properties of Poly(methyl methacrylate) thin films in supercritical carbon dioxide. *Macromolecules* **2002**, *35*, 1928−1935.
(13) Ogieglo, W.; Wormeester, H.; Eichhorn, K.-J.; Wessling, M.; Benes, N. E. In situ ellipsometry studies on swelling of thin polymer films: A review. *Prog. Polym. Sci.* **2015**, *42*, 42−78.
(14) Flichy, N. M. B.; Kazarian, S. G.; Lawrence, C. J.; Briscoe, B. J. An ATR−IR study of poly (dimethylsiloxane) under high-pressure carbon dioxide: Simultaneous measurement of sorption and swelling. *J. Phys. Chem. B* **2002**, *106*, 754−759.
(15) Guadagno, T.; Kazarian, S. G. High-pressure CO_2-expanded solvents: simultaneous measurement of CO_2 sorption and swelling of liquid polymers with in-situ near-IR spectroscopy. *J. Phys. Chem. B* **2004**, *108*, 13995−13999.
(16) Hopfenberg, H. B. *Permeability of plastic films and coatings*; Springer, 1974.
(17) Sanopoulou, M.; Roussis, P. P.; Petropoulos, J. H. A detailed study of the viscoelastic nature of vapor sorption and transport in a cellulosic polymer. I. Origin and physical implications of deviations from Fickian sorption kinetics. *J. Polym. Sci., Part B: Polym. Phys.* **1995**, *33*, 993−1005.
(18) Crank, J. *The mathematics of diffusion*; Oxford University Press: Oxford, UK, 1975.
(19) Loianno, V.; Bye, K. P.; Galizia, M.; Musto, P. Plasticization mechanism in polybenzimidazole membranes for organic solvent nanofiltration: Molecular insights from in situ FTIR spectroscopy. *J. Polym. Sci.* **2020**, *58*, 2547−2560.
(20) Mensitieri, G.; Scherillo, G.; Panayiotou, C.; Musto, P. Towards a predictive thermodynamic description of sorption processes in polymers: The synergy between theoretical EoS models and vibrational spectroscopy. *Mater. Sci. Eng.* **2020**, *140*, 100525.
(21) Pfefferle, W. C., Jr.; Goff, J. A.; Miller, J. G. Compressibility of gases. I. The Burnett method. An improved method of treatment of the data. Extension of the method to gas mixtures. *J. Chem. Phys.* **1955**, *23*, 509−513.
(22) *Thermophysical Properties of Fluid Systems*. website: https://webbook.nist.gov/chemistry/fluid/, accessed on June 10, 2020.
(23) Koros, W. J.; Paul, D. R. Design considerations for measurement of gas sorption in polymers by pressure decay. *J. Polym. Sci., Polym. Phys. Ed.* **1976**, *14*, 1903−1907.
(24) Turner, J. J. Quantitative Analysis. In *Handbook of Vibrational Spectroscopy*; Chalmers, J. M.; Griffiths, P. R. Eds. Wiley: Chichester, U.K., 2002, Vol. *1*, pp. 101−127.
(25) Siesler, H. W.; Ozaki, Y.; Kawata, H.; Heise, H. M. *Near-Infrared Spectroscopy. Principles, Instruments, Applications*; Wiley-VCH: Weinheim, Germany, 2002.
(26) *The symbols have the following meaning:* ν_1 = *symmetric stretching;* ν_2 = *bending;* ν_3 = *antisymmetric stretching.*
(27) Domanskaya, A. V.; Asfin, R. E.; Kyuberis, A. A.; Ebert, V. CH_4 broadening and shifting coefficients in the Fermi triad of $^{12}C^{16}O^2$ in the 2 μm region. *J. Quant. Spectrosc. Radiat. Transfer* **2019**, *235*, 209−216.
(28) Coleman, M. M.; Painter, P. C. Fourier transform infrared studies of polymeric materials. *J. Macromol. Sci., Part C* **1976**, *16*, 197−313.
(29) Koenig, J. L.; D'Esposito, L.; Antoon, M. K. The ratio method for analyzing infrared spectra of mixtures. *Appl. Spectrosc.* **1977**, *31*, 292−295.
(30) Griffiths, P. R.; de Haseth, J. A. *Fourier Transform Infrared Spectrometry*; John Wiley & Sons: New York, 1986.
(31) Turner, J. J. Bandwidths. In *Handbook of Vibrational Spectroscopy*; Chalmers, J. M.; Griffiths, P. R. Eds. John Wiley & Son: Chichester, UK, 2002, Vol. *1*, pp. 101−127.
(32) Clarke, J. H. R. Band Shapes and Molecular Dynamics in Liquids. In *Advances in Infrared and Raman Spectroscopy*; Clarke, J. H. R.; Hester, R. E. Eds. Heyden: London, 1978, Vol. *4*, pp. 109−193.
(33) Rothschild, W. G. Mobility of Small Molecules in Viscous Media. I. Rotational Motion of Methylene Chloride Molecules in Polystyrene by Far-Infrared Spectroscopy. *Macromolecules* **1968**, *1*, 43−47.
(34) Stolov, A. A.; Morozov, A. I.; Remizov, A. B. Infrared spectra and spinning diffusion of methyl bromide in solutions. *Vib. Spectrosc.* **1997**, *15*, 211−218.
(35) Wilson, E. B.; Decius, J. C.; Cross, P. C. *Molecular Vibrations*; McGraw-Hill: New York, 1955.
(36) Pope, D. S.; Koros, W. J.; Fleming, G. K. Measurement of thickness dilation in polymer films. *J. Polym. Sci., Part B: Polym. Phys.* **1989**, *27*, 1173−1177.
(37) De Angelis, M. G.; Merkel, T. C.; Bondar, V. I.; Freeman, B. D.; Doghieri, F.; Sarti, G. C. Hydrocarbon and fluorocarbon solubility and dilation in poly(dimethylsiloxane): comparison of experimental data with predictions of the Sanchez−Lacombe equation of state. *J. Polym. Sci., Part B: Polym. Phys.* **1999**, *37*, 3011−3026.

https://doi.org/10.1021/acs.iecr.1c00264
Ind. Eng. Chem. Res. 2021, 60, 5494−5503